34th Annual International Conference of the IEEE EMBS
San Diego, California USA, 28 August - 1 September, 2012

Extraction of Liver Vessel Centerlines under Guidance of Patient-Specific Models

Xishi Huang, Sameer Zaheer, Anwar Abdalbari, Thomas Looi, Jing Ren, and James Drake

Abstract— **Fast extraction of blood vessels of abdominal organs is still a challenging task especially in intra-procedural treatments due to large tissue deformation. In this study, we propose a novel joint vessel extraction and registration framework. This vessel extraction technique is under the guidance of prior knowledge patient specific models. The proposed technique automatically provides correspondence between extracted vessels and pre-procedural vessels, which is important for image guidance such as labeled vessels from pre-procedural models, improves the quality of disease diagnosis using multiple images and follow-up, and provides important information for nonrigid image registration. Another key component in our framework is to dynamically update mapped pre-procedural models by rapidly registering the patient model to the current image based on strain energy, point marks and 3D extracted vessels currently available.**

We have demonstrated the effectiveness of our technique in extraction of vessels from liver MR images. Validation shows a extraction error of 3.99 mm. This technique has the potential to significantly improve the quality of intra-procedural image guidance, diagnosis of disease and treatment planning.

I. Introduction

Vessel segmentation has many applications, including registration of pre-procedural images to intra-procedural images [1], delineating vascular territories in liver surgical planning [2], creating patient-specific simulations for optimizing radio-frequency ablation treatment and evaluating patient operability [3,4].

Blood vessels are often imaging targets in different imaging modalities such as magnetic resonance angiography (MRA), computed tomography angiography (CTA) and ultrasound as well. These vessel structures provide good references to localize treatment targets deep inside organs during treatment planning and treatment delivery, and prominent features to anchor deformable tissues to align two images together in image registration in order to reduce the chance of getting trapped in local minima. However, fast and accurate extraction of vessel centerlines is still a very challenging task. The most relevant vessel extraction techniques include ridge-based segmentation techniques [5,6] and template-based techniques [7,8]. Aylward et al. [5] described a ridge-based centerline tracking method that extracts centerlines. However, the method had two limitations. Firstly, the seed points were chosen to uniformly spanning the image, or by theshholding [5], thus leading to potentially long processing times [6]. Secondly, the procedure generated a disconnected set of centerlines, which were subsequently connected using straight cylinders between closest points on two disconnected vessels [9]. This procedure may not give an accurate localization of branch points. Additionally most centerline tracking algorithms require user interaction [10].

Under the guidance of prior patient specific models, we aim to develop a novel tracking-based segmentation technique for fast and accurate extraction of blood vessels inside the liver from magnetic resonance (MR) liver images. This new approach is based on joint extraction and registration of blood vessels. Specifically, correspondence between intermediate segmented vessels and pre-procedural patient-specific vessel models are employed to register the two images using a fast registration technique while dynamically updated registration results provide a better matched patient vessel model to more effectively guide vessel extraction. This technique is expected to have the capability to handle complex cases such as vessel branching and vessel touching/crossing caused by image artifacts or low image resolution. To meet strict time constraints during treatment procedures, this approach is able to extract only vessel branches required by specific procedures or specific region of interests (ROI).

To address the difficulty in localizing branch points in most tracking-based techniques, more accurate localization of bifurcation points is achieved by affine registration using local normalized cross-correlation (NCC) in the neighborhood of bifurcation.

The resulting vessel models can be employed for treatment planning, treatment delivery, and assessment of disease progression/regression, and facilitate image guidance in minimally invasive surgical procedures and noninvasive magnetic resonance (MR) guided high intensity focused ultrasound (HIFU) therapeutic procedures.

II. Methods and Materials

A. Joint Vessel Extraction and Registration Methodology

In this section, we present a joint vessel extraction and registration framework to rapidly extract the centerlines of blood vessels from MR liver images. The proposed

*Research supported by Canada Foundation for Innovation, Federal Economic Development Agency for Southern Ontario (SODA), and Ontario Research Foundation.

X. Huang is with the Department of Medical Imaging, University of Toronto and CIGITI, Hospital for Sick Children, 555 University Ave., Toronto, M5G 1X8, Canada (phone: 416-813-7654 x 28140; fax: 416-813-7477; e-mail: Edward.Huang@ sickkids.ca).

S. Zaheer, T. Looi, and J. Drake are with CIGITI, Hospital for Sick Children, 555 University Ave., Toronto, M5G 1X8, Canada.

A. Abdalbari and J. Ren is with the Faculty of Engineering and Applied Science, Univ. of Ontario Institute of Technology, 2000 Simcoe Street North, Oshawa, ON, L1H 7K4, Canada

technique automatically provides correspondence between extracted vessels and pre-procedural vessels as well.

The vessel extraction procedure is as follows. First, we perform initial match of the liver images using rigid transformation with N starting points, which is used to transform the patient-specific pre-procedural vessel model to current image space (called "guidance vessel model"). Next, using the guidance vessel model, vessel branches at the first level are extracted. To facilitate this extraction, the branch points at the level are automatically extracted using the local normalized cross-correlation method. Then, the newly extracted vessels are employed to register pre-procedural patient-specific vessel models using a fast vessel match technique to obtain a better match, which is used to update the guidance vessel model. This procedure is repeated until vessels at the last level in the guidance model are extracted. At each iteration, the registered vessels converge to the ground truth and thus the segmentation accuracy improves.

B. *Vessel Extraction*

The centerlines were extracted with the help of the guidance model. The guidance centerlines were divided into segments based on vessel tree structures, which were extracted from pre-procedural high quality MR images.

Seed generation: Each segment was extracted as shown in Fig. 1. First, a number of seeds are randomly (using a Mersenne-Twister uniform distribution) chosen in a region around starting point G1, the starting point of the guidance model, and the seed with the highest score (1) is selected.

$$\text{score} = (V^T G_{12})^2 / |S-G_1|, \qquad G_{12}=(G_2-G_1)/|G_2-G_1| \qquad (1)$$

where S is the seed point, and V is the eigenvector corresponding to the largest eigenvalue of the Hessian matrix computed at S. The numerator ensures the vessel with orientation closest to that of the guidance model is selected, while the denominator ensures that distant vessels oriented in the same direction as the guidance are not matched. The numerator is squared to give orientation matching more weight than distance.

Centerline tracking: Given that seed *S*, the centerline was extracted using a ridge-tracking algorithm as described by Aylward *et al*. [5]. Given a previous point (starting with the seed), the algorithm computes the Hessian matrix at that point. The eigenvector corresponding to the largest eigenvalue is taken as the direction of the vessel, while the other two eigenvectors form a plane representing the vessel cross-section. Next, the algorithm approximates the next point by moving in the direction of the vessel by a particular distance. Finally, the algorithm refines the estimation by finding the point of maximum intensity in the cross-section plane containing the approximation. The segment extraction terminates once the length of the extracted segment (T_1T_2) reaches the length of segment G_1G_2 in the guidance model.

Evaluating the segment: The dot product of the unit vectors of G_1G_2 and T_1T_2 is computed, and if greater than a threshold, the centerline extraction algorithm continues uninterrupted (and T_2T_3 will be extracted corresponding to G_2G_3). This will be true for the vast majority of segments. But this may not be true when the centerline tracking passes a branch point, and tracks the child branch not corresponding to the guidance model. In such a case the extracted segment will be discarded and the algorithm will try 2 remedies in succession: (I) if the segment was not initiated using seeds (e.g. T_2T_3), the algorithm will try to regenerate it using seeds; (II) but if step (I) has been tried or the segment was generated using seeds (e.g. T_1T_2), the segment will be skipped; (III) the algorithm will attempt to extract the next segment, and if successful, will replace the discarded segment with a straight line connecting the next segment with the previous one (if it exists).

After the curves of vessel centerlines are extracted from medical images, they are represented by smooth differential B-Spline curves to facilitate the fast registration technique.

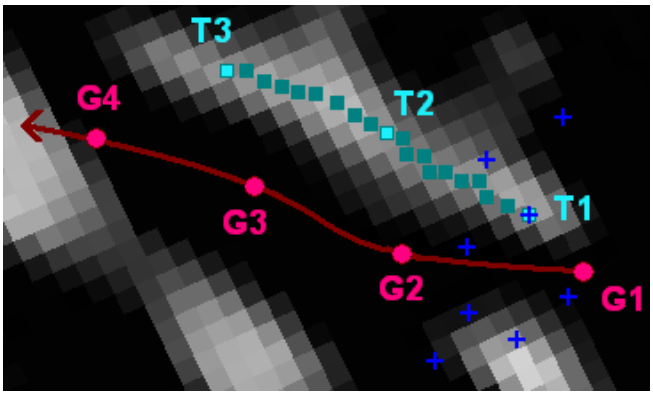

Figure 1. Illustration of the centerline extraction process. The red solid line is the guidance model, and points G_1 to G_4 delineate segments. The teal square points are those tracked by our centerline extraction method, and points T_1 to T_3 delineate the tracked segments. The blue '+' points are the seeds generated around G_1. The centerline extraction begins with the seed with the highest score (superimposed on T_1).

C. *Fast Registration to Update Guidance Model*

A good guidance model is an important component in our proposed vessel extraction technique. In order to rapidly update the guidance model, we need a fast registration technique to take full advantage of already extracted vessels. Based on elastic solid mechanics and the minimum strain energy principle, we recently proposed a fast method that gives an analytical optimal solution subject to constraints of 3D curves, point marks and strain energy. In this section, we briefly introduce the method. We aim to minimize the following energy function consisting of three terms:

$$J = w_e E_e(x) + w_c E_c(x) + w_m E_m(x) \qquad (2)$$

where $E_e(x)$ is strain energy produced by deformation of soft tissues, $E_c(x)$ the distance between pairs of 3D vessel centerlines extracted from the fixed and moving images, $E_m(x)$ the distance between corresponding point marks such as bifurcation points, and w_i weight relative importance of each term. This energy function measures the quality of alignment between two sets of blood vessels, i.e. vessels in the fixed image and the moving image respectively.

In this section, we provide a fast and robust analytical solution through specific design of different registration components.

Region-based transformation model: We adopt an adaptive neuro-fuzzy inference system (ANFIS) [11] to integrate region-based sub-models into a unified transformation model. Our neuro-fuzzy system has the following N_R rules:

Fuzzy rule *i*: If point *x* is in region R_i, then $x' = T_i(x)$

where *x* is a 3D point in the fixed image space, *x'* the corresponding transformed point, $T_i(x)$ a local transformation model specifically tailored to Region *i*. In summary, the overall transformation $T(x)$ can be derived as [12],

$$x' = T(x) = \sum_{i=1}^{N_R} M_i(x) T_i(x) \Big/ \sum_{i=1}^{N_R} M_i(x) \quad (3)$$

where $M_i(x)$ is the membership function of a fuzzy set associated with region R_i.

In this study, we choose linear transformation for each region, i.e. $T_i(x) = A_i x + b_i$. We can rewrite the overall transformation (3) for the whole image in the following form:

$$T(x) = A_p^T(x)\, p \quad (4)$$

where $p \equiv [\, p_{T1}^T \quad p_{T2}^T \quad \cdots \quad p_{TN_R}^T \,]^T$ is the total transformation parameters of $T(x)$, p_{Ti} is the corresponding 12 parameters (A_i, b_i) of $T_i(x)$. Note that transformation $T(x)$ is linear with respect to parameters *p*.

Shortest Distance of 3D Curves and its derivative with respect to transformation parameters: We propose a technique to analytically calculate the closest point on a 3D curve to a given point, and the derivative of the distance between curves with respect to transformation parameters through a parametric representation of 3D curves.

We aim to minimize the distance between pairs of corresponding vessel centerlines, which is formulated as minimizing the following function:

$$E_c(p) = \sum_{i=1}^{N_C} \sum_{k=1}^{N_{Ci}} \frac{1}{2} \left\| T(X_{fik}) - C_{mi}(t) \right\|^2 \quad (5)$$

where N_C is the total number of vessel centerlines, N_{Ci} the number of discrete points on the *i*-th centerline from the fixed image, $X_{fik}, i = 1,2,\cdots,N_C, k = 1,2,\cdots,N_{Ci}$ is the *k*-th point on the *i*-th centerline from the fixed image, $C_{mi}(t)$ the parametric representation of the *i*-th vessel centerline from the moving image. Its derivative is as follows.

$$\frac{\partial E_c(p)}{\partial p} = \sum_{i=1}^{N_C} \sum_{k=1}^{N_{Ci}} \frac{\partial E_{cik}}{\partial p} = \sum_{i=1}^{N_C} \sum_{k=1}^{N_{Ci}} \left\{ \left(\frac{\partial T}{\partial p}\right)^T \left(I_{3x3} - \left(\frac{\partial t}{\partial X_{fik}}\right) \left(\frac{\partial C_{mi}(t)}{\partial t}\right)^T \right) \left(X_{Tfik} - X_{cmik}(t_{cmik}) \right) \right\} \quad (6)$$

$$= \sum_{i=1}^{N_C} \sum_{k=1}^{N_{Ci}} \left\{ A_p(X_{Tfik}) D_{cmik}^T A_p^T(X_{Tfik}) \right\} p - \sum_{i=1}^{N_C} \sum_{k=1}^{N_{Ci}} \left\{ A_p(X_{Tfik}) D_{cmik}^T X_{cmik} \right\}$$

Note that $\frac{\partial E_c(p)}{\partial p}$ is a linear function of transformation parameters *p*, which implies that the distance between curves $E_c(p)$ is a quadratic function of parameters *p*.

Minimum Strain Energy: The strain energy term prevents the issue of overfitting (for example, physically impossible deformation), and leads to physically consistent deformable match results. Strain energy $E_{e(x)}$ is generated by deformation of soft tissues based on elastic solid mechanics, and can be calculated using the Saint-Venant model [13], as follows:

$$E_e = \iiint_{\Omega} W(E)\, dxdydz \quad , \quad (7)$$

$$W(E) = 0.5\lambda \left(tr(E)\right)^2 + \mu\, tr(E^2) \;,\; tr(E) \equiv e_{11} + e_{22} + e_{33}$$

where $W(E)$ is the strain energy density, (λ, μ) tissue elastic parameters, E a strain tensor, $E = \left(e_{ij}\right)_{3x3}$, $e_{ij} \approx \frac{1}{2}\left(\frac{\partial T_i}{\partial x_j} + \frac{\partial T_j}{\partial x_i} - 2\delta_{ij} \right)$.

From (4), we write strain energy as a quadratic function of our proposed neuro-fuzzy transformation parameters *p* in the following formula:

$$E_e(p) = C_{e0} + C_{e1}^T p + p^T C_{e2} p \quad (8)$$

$$C_{e0} = \iiint_{\Omega} C_0(x)\, dxdydz \;,\; C_{e1} = \iiint_{\Omega} C_1(x)\, dxdydz \;,$$

$$C_{e2} = \iiint_{\Omega} C_2(x)\, dxdydz \;,\; W(E) = C_0(x) + C_1^T(x) p + p^T C_2(x) p$$

where constants (C_{e0}, C_{e1}, C_{e2}) can be calculated offline in advance based on the pre-procedural image.

Point marks: Point marks are employed to anchor the deformation at some specific locations. Point marks such as bifurcations provide the most robust and efficient way to obtain correct registration. We assume that there are N_m pairs of corresponding point marks (i.e. bifurcation points), $\left(X_{fk}, X_{mk}\right), k = 1,2,\cdots,N_m$. Then we minimize the distance between corresponding point marks by adding the following term to the registration energy function,

$$E_m(p) = \sum_{i=1}^{N_m} \frac{1}{2} \left\| T(X_{fk}) - X_{mk} \right\|^2 \quad (9)$$

Its derivative with respect to transformation parameters can be analytically calculated through the following formula,

$$\frac{\partial E_m(p)}{\partial p} = \sum_{i=1}^{N_m} A_p(X_{fk}) \left(T(X_{fk}) - X_{mk} \right) \quad (10)$$

From the above derivation, all the terms are quadratic functions of transformation parameters *p*. Therefore, the global optimal transformation parameters can be calculated analytically by solving linear equations $\partial J / \partial p = 0$.

This fast analytical solution is used to transform the pre-procedural model to obtain the guidance vessel model.

D. NCC Registration Based Accurate Localization of Bifurcation Points

In a ridge-tracking based technique, it is difficult to effectively localize bifurcation points. In this study, we employ an image registration method to localize bifurcations. Specifically, after we update the guidance model based on latest extracted vessel segments, if there exist, the branch points in the guidance model corresponding to the latest extracted vessels are expected in the neighborhood of corresponding bifurcations in the image. Within a window size, local NCC is used to register the two images, then we employ the resulting optimal affine transformation to transform the bifurcation point in the guidance model to current image space, which is expected as the accurate location of corresponding branch point associated with the vessel segments.

III. Experimental Results

All of the images used in this study were acquired from human volunteers. High-quality dynamic MR images were acquired in the axial plane using a 1.5T GE scanner (GE Medical Systems, Milwaukee, WI). Image acquisition was performed using the LAVA gradient echo sequence with TR=3.79 ms, TE=1.72ms, a flip angle of 12 degrees, an image matrix size of 256 x 256, in-plane pixel size of 1.3 mm x 1.3 mm and slice thickness = 1.5 mm. Image sets were acquired with a breath-hold at different positions.

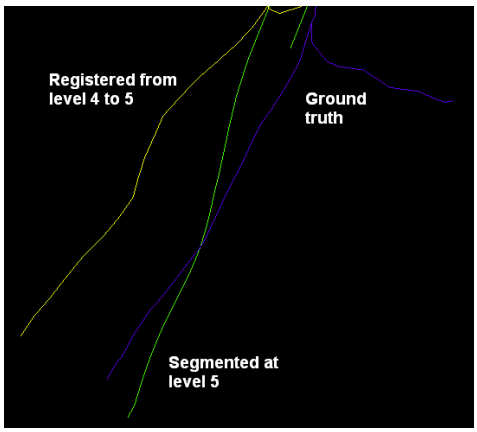

Figure 2. Extracted centerlines. Purple lines: gold standard centerlines by VMTK, yellow lines: guidance model, green lines: extracted by our method.

The pre-procedural vessels were extracted from one MR image by open source VMTK with extensive user intervention. Under the guidance of the pre-procedural vessel model, vessels were extracted from the second MR image using our proposed method. The extracted vessels and gold standard vessels (extracted by VMTK) are shown in Fig. 2.

To quantitatively evaluate the extraction accuracy, we calculated average centerline distance (ACD) between extracted vessels and those obtained by VMTK. The resulting ACD is 3.99 mm. These results have demonstrated that the proposed vessel extraction technique is able to automatically extract the vessels from MR images given starting points and automatically provide the correspondences of vessels in two images. The run-time for extracting 102 vessel branches of the image was 34 seconds. The algorithm was written in C++ and run on a computer running Microsoft Windows XP with a 3.2-GHz i3 processor and 3.5 GB of memory.

IV. Discussion and Conclusion

We propose a novel joint vessel extraction and registration framework. The proposed technique provides not only centerlines of blood vessels but also automatic correspondence information between extracted vessels and the pre-procedural model, which allows us to extract vessels labeled in the pre-procedural model. The technique also provides important information for nonrigid image registration.

We have demonstrated the effectiveness of our technique in extraction of vessels from liver MR images. This technique has the potential to significantly improve the quality of intra-procedural image guidance, disease diagnosis using multiple images (including follow-ups), and treatment planning.

Future work includes parallel implementation of our algorithm to accelerate the extraction process, more validation on clinical data, and integration into clinical procedures at our hospital.

References

[1] Nam, W.H. et al., "Automatic registration between 3D intra-operative ultrasound and pre-operative CT images of the liver based on robust edge matching," Phys. Med. Biol., vol. 57, no. 2012, pp. 69–91, Nov 2011.

[2] Selle, D. et al., "Analysis of Vasculature for Liver Surgical Planning," IEEE Trans. Med. Imag. vol. 21, pp. 1344-1357, Nov. 2002.

[3] Payne, S. et al., "Image-based multi-scale modelling and validation of radio-frequency ablation in liver tumours," Philos Transact A Math Phys Eng Sci. vol. 369, no. 1954, pp. 4233-54, Nov. 2011.

[4] Eiheim, O.C.. "Segmentation of liver vessels as seen in MR and CT images," CARS 2004: COMPUTER ASSISTED RADIOLOGY AND SURGERY, vol. 1268, pp. 201-206, 2004.

[5] Aylward, S. R., "Initialization, noise, singularities, and scale in height ridge traversal for tubular object centerline extraction," IEEE Transactions on Medical Imaging, vol. 21, no. 2, pp. 61-75 2002

[6] Bullitt, E. et al., "Analyzing attributes of vessel populations," Medical Image Analysis, vol. 9, no. 1, pp. 39-49, 2005.

[7] R.R. Petrocelli, et al. "A new method for structure recognition in unsubtracted digital angiograms," Proceedings of Computers in Cardiology, pp. 207-210, October 1992.

[8] Q. Lin, *Enhancement, Detection, and Visualization of 3D Volume Data*. Ph.D. Thesis, Dept. EE, Linköping University, Sweden, May 2003.

[9] E. Bullitt, E. et al,. "Symbolic description of intracerebral vessels segmented from magnetic resonance angiograms and evaluation by comparison with X-ray angiogram," Medical Image Analysis, vol. 5, no. 2, pp. 157-169, 2001.

[10] D. Lesage et al., "A review of 3Dvesel lumen segmentation techniques: Models, features and extraction schemes," Medical Image Analysis, vol. 13, no. 6, pp. 819-845, 2009.

[11] R.J.S. Jang, "ANFIS: adaptive-network-based fuzzy inference system," IEEE Trans Syst Man Cybern 23, pp. 665-685, 1993.

[12] X. Huang, et al., "A soft computing framework for software effort estimation," Soft Computing 10, pp. 170-177, 2006.

[13] P.G. Ciarlet, *Mathematical Elasticity*, vol. 1, North Holland, 1988.